

Latency-Gated Coherent Emission with Anchored Memory Scales: A Non-Markovian Effective Model for ASKAP J1832–0911

Darío Peyrú¹

¹*Independent Researcher, Pilar, Buenos Aires, Argentina*

ASKAP J1832–0911 is an unusually bright long-period transient showing strictly periodic, phase-locked radio and X-ray emission with period $P \simeq 44.2$ min and minute-scale “on” windows. This phenomenology is difficult to reproduce in purely instantaneous gating models and motivates an effective description with thresholded dissipation and internal memory. We present a revised non-Markovian phenomenology, structurally aligned with the memory-kernel upgrade of MetaTime v36.2 but recast here as a compact-object emission model rather than as a cosmological closure. The central dynamical variable $q(t)$ is interpreted as a coarse-grained magnetospheric coherence/current-closure parameter for the emitting region, while a latent state $m(t)$ tracks the delayed build-up of dissipative load. The governing kernel is the minimal causal exponential law $\dot{m} = (\Pi - m)/\tau_m$, and the observed burst gating is generated by a threshold crossing of $q(t)$ under periodic driving. Relative to the earlier version, the present manuscript (i) specifies the physical role of q , (ii) identifies the effective latency rate Γ_L and memory time τ_m with mesoscale reorganization times of the emitting zone, (iii) keeps Landauer bookkeeping only as a diagnostic consistency relation, not as a direct constraint, and (iv) derives approximate links between the model parameters and the observed onset phase, critical gating threshold, and duty-cycle scale. A reproducible toy integration exhibits a critical Γ_L separating bursting from quiescence and a finite- τ_m phase lag that provides a falsifiable hysteresis signature. The model remains phenomenological, but it is now better anchored to compact-object timescales and more clearly testable with continued monitoring.

I. OBSERVATIONAL SCOPE AND MODELLING TARGET

ASKAP J1832–0911 is a high-value target within the growing class of long-period transients (LPTs). It shows correlated radio and X-ray emission, a stable period of about 44.2 min, and narrow active windows of order minutes rather than a large fraction of the cycle. The leading astrophysical interpretations currently involve an old magnetar or an ultra-magnetized white dwarf, but no consensus microphysical model yet explains simultaneously the long period, the phase-locked multiwavelength activity, and the strongly intermittent duty cycle. The present paper does *not* attempt to replace detailed compact-object magnetospheric modelling. Instead, it asks whether a minimal non-Markovian effective description can capture the observed phenomenology while producing a genuinely new signature absent from memoryless gating models.

The conceptual import from MetaTime v36.2 is narrow and structural. In v36.2, the dark-sector exchange gains an internal clock through an exponential memory kernel. Here, the same mathematics is used to model delayed dissipation in a compact-object emission zone. The claim is therefore not that the pulsar is “explained by cosmology,” but that the same causal kernel may be a useful effective tool in two very different contexts.

II. PHYSICAL INTERPRETATION OF THE REDUCED VARIABLE

The main weakness of the earlier draft was that the reduced coordinate $q(t)$ was left too abstract. In the present revision, q is defined as a *dimensionless coherence/current-*

closure parameter for the emitting zone. Operationally, q measures how close the local magnetospheric state is to a configuration capable of sustaining the coherent radio/X-ray-active manifold. One may think of it as a coarse-grained order parameter combining current closure, pair-loading support, and field-line organization in the emission region. It is not a directly observed quantity, and it is not claimed to be unique. Its purpose is to parametrize a thresholded state variable whose excursions above q_c open the burst window.

A minimal effective Lagrangian is

$$L(q, \dot{q}, t) = \frac{1}{2} M \dot{q}^2 - V(q) + J(t)q, \quad (1)$$

with an effective double-well or tilted metastable potential

$$V(q) = \frac{\lambda}{4} (q^2 - q_0^2)^2 + \frac{\kappa}{2} q^2, \quad (2)$$

where the κ term represents ordinary linear leakage out of the coherent manifold and the quartic term provides metastability between off and on sectors. We do not claim that Eq. (2) is the literal magnetospheric potential. It is the simplest effective shape that justifies using a thresholded order parameter with an overdamped reduction.

The external periodicity is represented by a drive

$$J(t) = \frac{J_0}{2} \left[1 + \sin \left(\frac{2\pi t}{P} \right) \right], \quad (3)$$

where $P \simeq 2652$ s is fixed by observation. The drive stands in for the slowly modulated forcing associated with rotation, precession, orbital sweeping, or another coherent periodic agent. Again, the EFT does not choose among these microphysical origins; it only inherits their periodicity.

III. NON-MARKOVIAN LOAD AND ANCHORED TIMESCALES

The central non-Markovian ingredient is a latent load variable $m(t)$ obeying

$$\dot{m}(t) = \frac{1}{\tau_m} \left(\Pi[q(t)] - m(t) \right), \quad (4)$$

with the proxy chosen as

$$\Pi(q) = 1 + \left(\frac{q}{q_c} \right)^2. \quad (5)$$

The dissipation functional is taken to be

$$\mathcal{R}[q, \dot{q}; m] = \frac{1}{2} \Gamma_L m(t) \dot{q}^2, \quad (6)$$

so that larger delayed load increases friction against coherent reconfiguration. The resulting dissipative Euler–Lagrange equation is

$$\frac{d}{dt} \left(\frac{\partial L}{\partial \dot{q}} \right) - \frac{\partial L}{\partial q} = - \frac{\partial \mathcal{R}}{\partial \dot{q}}, \quad (7)$$

which yields

$$M \ddot{q} + \frac{dV}{dq} - J(t) = -\Gamma_L m(t) \dot{q}. \quad (8)$$

The important improvement over the earlier draft is that τ_m and Γ_L are now interpreted as *mesoscale* parameters of the emitting region. They are not microscopic plasma times such as the light-crossing time or gyrotime. Rather, they encode the effective reorganization time of pair-loading and current closure in the active zone after coarse-graining over many local degrees of freedom. This distinction matters because the observed on-windows are of order minutes, whereas microscopic magnetospheric times are far shorter. The EFT statement is therefore that the relevant gating dynamics operate at a collective, not microscopic, level.

A practical anchor follows from timescale matching. In the strongly damped regime, the rise into the coherent manifold is set by

$$\tau_{\text{rise}} \sim (\kappa + \Gamma_L m)^{-1}. \quad (9)$$

Minute-scale onsets imply

$$\kappa + \Gamma_L m = O(10^{-3} - 10^{-2}) \text{ s}^{-1}, \quad (10)$$

which immediately places the phenomenological latency rate in the same range as the toy threshold table, rather than leaving it wholly unconstrained. Likewise, finite-memory signatures become visible only when

$$\tau_m / P \gtrsim 10^{-3}, \quad (11)$$

but are washed out for $\tau_m \ll P$; thus values from seconds to a few hundred seconds are the natural phenomenological target if one wishes to see phase-lag effects in a 44.2-minute cycle.

IV. OVERDAMPED REDUCTION AND BURST THRESHOLD

For emission gating the overdamped regime is the useful limit. Neglecting $M \ddot{q}$ and linearizing the quartic potential near the relevant branch gives the reduced system

$$\dot{q} = J(t) - (\kappa + \Gamma_L m) q, \quad (12)$$

$$\dot{m} = \frac{1}{\tau_m} (\Pi(q) - m). \quad (13)$$

Coherent emission is declared active when

$$q(t) \geq q_c. \quad (14)$$

This construction is simpler than a full magnetospheric instability calculation but still produces an observable duty cycle,

$$D = \frac{\tau_{\text{on}}}{P}. \quad (15)$$

In the quasi-static near-Markovian limit $m \simeq 1$, the instantaneous steady state is

$$q_{\text{ss}}(t) \simeq \frac{J(t)}{\kappa + \Gamma_L}. \quad (16)$$

Threshold crossing requires

$$J(t) \geq J_{\text{th}} \equiv q_c (\kappa + \Gamma_L \bar{m}), \quad (17)$$

where \bar{m} denotes the cycle-averaged latent load in the near-threshold regime. Thus the onset phase and approximate active window are controlled by the ratio J_{th}/J_0 . Writing

$$s \equiv \frac{2J_{\text{th}}}{J_0} - 1, \quad -1 < s < 1, \quad (18)$$

the fraction of one cycle spent above threshold in the quasi-static approximation is

$$D_{\text{qs}} \simeq \frac{1}{2} - \frac{1}{\pi} \arcsin s. \quad (19)$$

Equation (19) is not a substitute for integrating Eq. (13), but it makes the population-level prediction explicit: broader active windows correspond to smaller effective barriers $\kappa + \Gamma_L \bar{m}$, while sources close to quiescence sit at $s \rightarrow 1^-$ and are most sensitive to small secular changes in Γ_L or τ_m .

This addresses one of the main criticisms of the first version. The period P remains observational input, but the burst window is no longer a purely imposed feature: it emerges from threshold crossing against a load-dependent damping rate.

V. BENCHMARK INTEGRATION AND CRITICAL LATENCY

To keep the model reproducible, we adopt a benchmark normalization close to the earlier draft,

$$P = 2652 \text{ s}, \quad q_c = 0.05, \quad J_0 = 3.5 \times 10^{-4}, \quad (20)$$

TABLE I. Benchmark integration of Eq. (13) for $\tau_m = 1$ s. A burst is recorded if $q(t)$ crosses q_c at least once within one cycle.

Γ_L (s^{-1})	Burst?	First crossing (s)
0	yes	278
1×10^{-3}	yes	342
2×10^{-3}	yes	488
3×10^{-3}	no	—
4×10^{-3}	no	—

with $\kappa = 2 \times 10^{-3} s^{-1}$, timestep $\Delta t = 2$ s, and initial data $q(0) = 0$, $m(0) = 1$. These values are not claimed as fitted source parameters. They are chosen to place the system near threshold, where finite memory has visible consequences.

Table I shows the first threshold crossing as a function of Γ_L in the near-Markovian regime. A critical interval appears between roughly 2×10^{-3} and $3 \times 10^{-3} s^{-1}$, beyond which bursting is lost in the benchmark realization. This is the main quantitative output of the toy model.

Figure 1 shows two concrete non-Markovian signatures. At fixed $\Gamma_L = 2 \times 10^{-3} s^{-1}$, increasing τ_m from 1 s to 300 s shifts the phase of threshold crossing and changes the trajectory near the on-manifold. The right panel shows how the first threshold crossing varies with Γ_L for the two memory times. As expected, the curves remain close when the system is comfortably above threshold, because the gating is then controlled primarily by the drive amplitude and the baseline leak. The finite-memory correction becomes observationally important only near the critical regime, where a small lag in $m(t)$ changes whether and when the trajectory crosses $q = q_c$. This is the compact-object analogue of the hysteresis kill test used in the cosmological closure: identical instantaneous forcing can yield different effective dissipation depending on the system's retained history.

VI. ENERGETIC BOOKKEEPING AND WHAT LANDAUER CAN – AND CANNOT – DO

The dissipative power associated with the latency term is

$$\dot{E}_{\text{proc}} = \Gamma_L m(t) \dot{q}^2 \geq 0. \quad (21)$$

This quantity is useful because it ties the gating dynamics to an explicit energy sink. However, the previous draft overstated the role of Landauer as a direct astrophysical constraint. The correct statement is weaker. If an independent estimate of an effective bath temperature T_{eff} for the active region is available, then one may write the diagnostic inequality

$$\dot{N}_{\text{erase}} \leq \frac{\dot{E}_{\text{proc}}}{k_B T_{\text{eff}} \ln 2}. \quad (22)$$

Equation (22) is therefore bookkeeping, not a stand-alone constraint. In the absence of a separately anchored T_{eff} , it does not by itself rule in or rule out a parameter set. What it does provide is a dimensional consistency check once a candidate magnetospheric environment is specified. This is the level at which Landauer should appear in the present paper.

VII. FALSIFIABLE PREDICTIONS AND NEXT-STEP DISCRIMINATION

The revised model retains the strongest predictions of the earlier draft while stating their scope more carefully.

(P1) *Critical-quiescence transition.* If the effective latency rate drifts upward, the source should not fade continuously but should cross a relatively sharp threshold from burst-capable to quiescent behavior, analogous to Table I.

(P2) *Phase-lag response.* Slow changes in the emission environment that preserve the period P can still shift burst onset because finite τ_m changes the delayed load. This effect vanishes in the Markovian limit.

(P3) *Onset/decay asymmetry.* Because the memory variable does not instantaneously track $\Pi(q)$, the approach to the on-state and the retreat from it need not be time-reversal symmetric even under the same periodic drive. This is the cleanest hysteresis prediction.

(P4) *Radio/X-ray co-modulation.* If Eq. (21) tracks the dissipative activity of the coherent zone, then phases of strongest radio coherence should coincide with enhanced dissipative channels, broadly consistent with phase-locked X-ray behavior.

(P5) *Population test.* Across the LPT class, sources with broader active windows should preferentially correspond to smaller values of the effective barrier $\kappa + \Gamma_L \bar{m}$, with the quasi-static scaling $D \approx D_{\text{qs}}(J_{\text{th}}/J_0)$ from Eq. (19). In particular, sources near the quiescent threshold $s \rightarrow 1^-$ should show the strongest sensitivity to small secular shifts in Γ_L or τ_m , whereas sources far from threshold should be comparatively insensitive to memory.

The decisive next step is not conceptual but observational: combine long-baseline monitoring with source-class priors to test whether onset phase and quiescent intervals exhibit the predicted history dependence.

VIII. CONCLUSION

This revised pulsar/LPT paper keeps the useful part of the original proposal and removes what was too loose. The useful part is the non-Markovian kernel: the same minimal causal memory law that proved fruitful in the cosmological setting naturally generates delayed dissipation and phase-lag effects in a compact-object gating problem. What was too loose was the physical anchoring. In the present version, the reduced coordinate q is interpreted as a magnetospheric coherence/current-closure

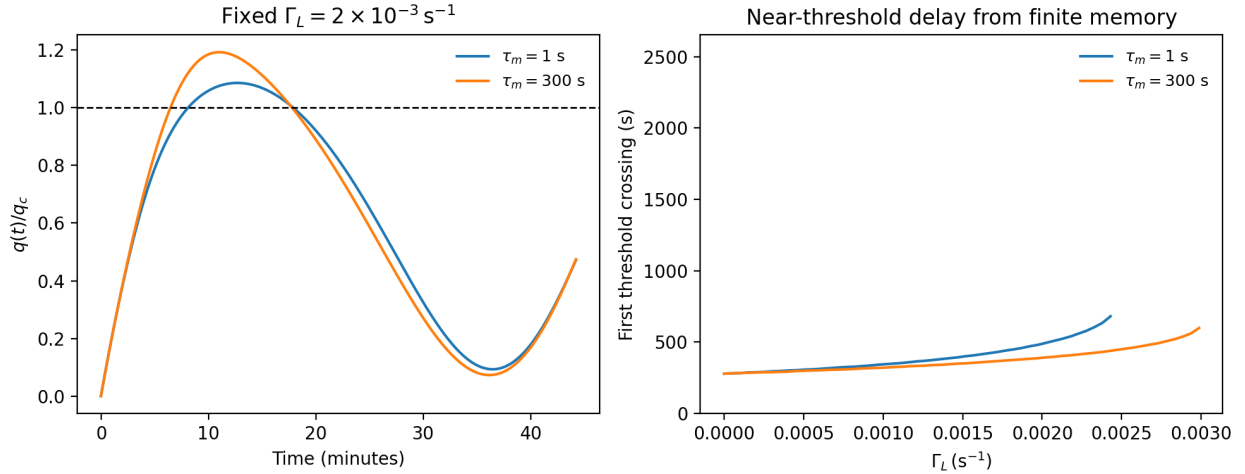


FIG. 1. Left: normalized gating trajectories $q(t)/q_c$ at fixed $\Gamma_L = 2 \times 10^{-3} \text{ s}^{-1}$ for a near-Markovian case ($\tau_m = 1 \text{ s}$) and a finite-memory case ($\tau_m = 300 \text{ s}$). Right: first threshold crossing as a function of Γ_L for the same two memory times. The memory kernel shifts onset phase and modifies the critical approach to quiescence. These are benchmark integrations of Eq. (13), not fits.

order parameter, the latency rate Γ_L is tied to minute-scale reorganization of the active region, and the memory time τ_m is treated as a mesoscale relaxation time that can plausibly range from seconds to hundreds of seconds without being forced into microscopic plasma values.

The result is still a phenomenological EFT, not a first-principles magnetospheric solution. But it is now better

posed. It derives a threshold condition, exhibits a critical latency scale, clarifies the limited role of Landauer bookkeeping, and preserves a genuinely new prediction: a hysteretic asymmetry between onset and decay in the burst cycle. ASKAP J1832–0911 remains a direct observational anchor, and continued monitoring can now test a sharper claim: not merely whether the source is periodically gated, but whether its gating remembers.

-
- [1] Z. Wang, N. Rea, T. Bao, D. L. Kaplan, E. Lenc, Z. Wadasingh, *et al.*, “Detection of X-ray emission from a bright long-period radio transient,” *Nature* **642**, 583–586 (2025).
 - [2] N. Hurley-Walker, X. Zhang, A. Bahramian, *et al.*, “A radio transient with unusually slow periodic emission,” *Nature* **601**, 526–530 (2022).
 - [3] N. Hurley-Walker, N. Rea, S. J. McSweeney, *et al.*, “A long-period radio transient active for three decades,” *Nature* **619**, 487–490 (2023).
 - [4] M. Caleb, E. Lenc, D. L. Kaplan, *et al.*, “An emission-state-switching radio transient with a 54-minute period,” *Nature Astronomy* **8**, 1159–1168 (2024).
 - [5] R. Landauer, “Irreversibility and Heat Generation in the Computing Process,” *IBM Journal of Research and Development* **5**, 183–191 (1961).